EXPERIMENTAL INVESTIGATION ON COOLING PERFORMANCE OF SYNTHETIC JET

M.Tech. Thesis

By

KARTIK KUMAR GUPTA

(Roll.: 2302103054)

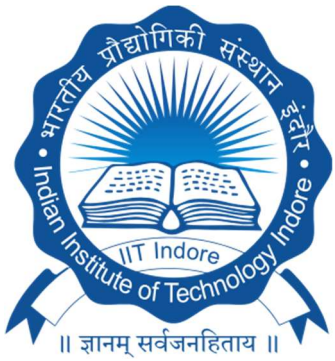

DEPARTMENT OF MECHANICAL ENGINEERING

INDIAN INSTITUTE OF TECHNOLOGY INDORE

JUNE 2025

EXPERIMENTAL INVESTIGATION ON COOLING PERFORMANCE OF SYNTHETIC JET

A THESIS

Submitted in partial fulfillment of the requirements for the award of the degree
of
Master of Technology

by
KARTIK KUMAR GUPTA

DEPARTMENT OF MECHANICAL ENGINEERING
INDIAN INSTITUTE OF TECHNOLOGY INDORE
JUNE 2025

INDIAN INSTITUTE OF TECHNOLOGY INDORE

CANDIDATE'S DECLARATION

I hereby certify that the work which is being presented in the thesis entitled "**EXPERIMENTAL INVESTIGATION ON COOLING PERFORMANCE OF SYNTHETIC JET"** in the partial fulfillment of the requirements for the award of the degree of **MASTER OF TECHNOLOGY** and submitted in the **Department OF Mechanical Engineering, Indian Institute of Technology Indore**, is an authentic record of my own work carried out during the time period from July 2025 to June 2025 under the supervision of **Prof. Santosh Kumar Sahu, Indian Institute of technology Indore.**

The matter presented in this thesis has not been submitted by me for the award of any other degree of this or any other institute.

Kartik
18-06-25

Signature of the student with date
(KARTIK KUMAR GUPTA)

This is to certify that the above statement made by the candidate is correct to the best of my/our knowledge.

18.06.2025

Signature of the Supervisor of M.Tech. thesis with date
(Prof. SANTOSH KUMAR SAHU)

KARTIK KUMAR GUPTA has successfully given his/her M.Tech. Oral Examination held on 26/05/2025.

Signature of Supervisor of M.Tech. thesis
Date:18.06.2025

Convener, DPGC
Date: 19-06-2025

ACKNOWLEDGEMENTS

I would like to express my heartfelt gratitude to my thesis supervisor**, Prof. Santosh Kumar Sahu**, for his invaluable guidance, support, and continuous encouragement throughout the course of this research. His expertise, insightful feedback, and unwavering patience played a pivotal role in shaping this thesis into its present form.

I extend my sincere thanks to **Prof. Shanmugan Dhinakaran**, Head of the Department of Mechanical Engineering, for fostering an environment conducive to learning and research. I am also grateful to **Prof. Suhas Joshi**, Director of IIT Indore, for providing world-class infrastructure and academic resources that enriched my academic journey.

I would like to thank **Dr. Pawan Sharma** for his help and support during the experimental work. My deepest appreciation goes to my friends and peers who stood by me through the highs and lows of this endeavour. I would especially like to thank **Prithviraj Soni, Anshul Kashyap, Kushagra Parihar, and Prashant Singh** for their constant support, insightful discussions, and motivation throughout this period. I would also like to thank **Arun Kumar Bhagwaniya** for his contributions and assistance during various stages of this work.

I am sincerely thankful to all the faculty members and staff of the Department of Mechanical Engineering at IIT Indore for their technical assistance and moral support during my M.tech. program.

Lastly, I am profoundly grateful to my family for their unconditional love, encouragement, and belief in me, without which this work would not have been possible.

-Kartik Kumar Gupta

“Dedicated to My Parents for Their Love, Support & Blessings.”

ABSTRACT

This thesis focuses on the experimental evaluation of synthetic jets (SJs) for thermal management in compact electronic systems. Synthetic jets, characterized by their zero-net mass flux operation and compact design, offer promising advantages for efficient heat dissipation without the need for external fluid supply. The study investigates the impact of elliptical orifice shapes with varying aspect ratios (AR = 1 to 14) on cooling performance during jet impingement. A custom-built test facility was employed, comprising an SJ actuator, stainless steel test surface, power oscillator, DC power supply, and a traversing mechanism to position the actuator at varying distances. Surface temperature distributions were recorded using a thermal imaging camera (FLIR A655sc), allowing for detailed analysis of heat transfer behaviour. The results highlight those elliptical jets, especially those with an aspect ratio of 10, deliver enhanced cooling performance due to improved flow spreading and vortex interactions. These outcomes provide useful insights for the design of efficient, space-constrained thermal management solutions.

.

CONTENTS

Abstract i
List of Figures iv
List of Tables v

Nomenclature vi
Abbreviations vii

1.Introduction 1
1.1 Background 1
1.2 Classification of Cooling Technologies 2
1.3 Synthetic Jets 3
1.4 Motivation 6
1.5 Objectives of the Project 7
1.6 Application of Synthetic Jet 7

2.Literature Review 9
2.1 Overview 9
2.2 Cooling Technologies Overview 10
2.3 Characteristics of Synthetic Jets 10
2.3.1 Axis Switching Phenomenon 11
2.4 Gaps Identified in Literature 11

3.Experimental Methodology 13
3.1 Overview 13
3.2 Experimental Setup 13
3.2.1 Synthetic Jet Actuator 14
3.2.2 Orifice Plates 14
3.2.3 Orifice Design and Aspect Ratio details 15
3.2.4 Test Surface 16
3.2.5 Traversing Mechanism 17
3.3 Measurement and Instrumentation 17
3.3.1 Temperature Measurement 17
3.3.2 Data Aquisition 17
3.4 Test Conditions 17

3.5 Data Processing and Calculations 18
3.5.1 Heat Transfer Coefficient 18

4.Result and discussion 20
4.1 Effect of Jet-to-Surface Distance (z/d) 20
4.1.1 Heat Transfer Performance at z/d = 1 20
4.1.2 Heat Transfer Performance at z/d = 3 21
4.1.3 Heat Transfer Performance at z/d = 6 22
4.1.4 Heat Transfer Performance at z/d = 10 23
4.1.5 Heat transfer performance along both the major and minor axes of the elliptical synthetic jet at various z/d ratios and aspect ratios (AR). 24
4.2 Surface Temperature Distribution 26
4.2.1 Temperature distribution contour 26
4.3 Influence of Aspect Ratio (AR) 29

5.Conclusion and future Scope 30
5.1 Conclusion & Future Scope

References 32
Appendix 33

LIST OF FIGURES

Fig.1.1 Various cooling technologies for thermal management of electronics 2

Fig.1.2 Schematic of synthetic jet during a) ingestion stroke b) expulsion stroke 3

Fig.1.3 Parameters affecting synthetic jet 4

Fig.1.4 Schematic evolution of synthetic jet with different regions 5

Fig.3.1 Experimental set up 13

Fig.3.2 Schematic view of different aspect ratio orifice 15

Fig.3.3 Schematic of heating plate assembly used for heat transfer study in present investigation. 16

Fig.4.1 Nusselt number vs radial location (r/d) at z/d = 1 20

Fig.4.2 Nusselt number vs radial location at z/d = 3 21

Fig.4.3 Nusselt number vs radial location at z/d = 6 22

Fig.4.4 Nusselt number vs radial location at z/d = 10 23

Fig.4.5 Variation of Nusselt number along (a) major axis and (b) minor axis for different orifice aspect ratios (AR = 1–14). 24

Fig.4.6 Contour map of temperature distribution for different elliptical aspect ratio orifice at dimensionless spacing z/d = 1 27

Fig.4.7 Contour map of temperature distribution for different elliptical aspect ratio orifice at dimensionless spacing z/d = 3 27

Fig.4.8 Contour map of temperature distribution for different elliptical aspect ratio orifice at dimensionless spacing z/d = 6 28

Fig.4.9 Contour map of temperature distribution for different elliptical aspect ratio orifice at dimensionless spacing z/d = 10 28

LIST OF TABLES

Table.1.1 Variable geometric and operational parameters used in current study 14

Table.1.2 Design parameters of different elliptical aspect ratio orifices 15

Table.1.3 Dimension of thermo-physical properties of test surface 16

NOMENCLATURE

A	Area of test surface (mm²)
Ar_o	Orifice area (mm²)
b	Slot width (mm)
d	Orifice diameter (mm)
d_e	Equivalent diameter of orifice (mm)
d_h	Hydraulic diameter of orifice (mm)
D	Diaphragm diameter (mm)
E	Voltage across the hot wire probe (V)
f	Actuation frequency (Hz)
f_d	Diaphragm resonance frequency (Hz)
f_h	Helmholtz resonance frequency (Hz)
h	Local heat transfer coefficient (W/m²·K)
h_{avg}	Average heat transfer coefficient (W/m²·K)
$h_{e_{ff},b}$	Effective heat transfer coefficient from back surface (W/m²·K)
H	Cavity depth (mm)
I	Current through test foil (A)
k	Thermal conductivity of test surface (W/m·K)
k_f	Thermal conductivity of fluid (W/m·K)
K	Jet formation constant

L_0	Stroke length (mm)
Nu	Local Nusselt number (hd/ k_f)
Nu_0	Stagnation point Nusselt number (hd/ k_f)
Nu_{avg}	Average Nusselt number
P_a	Atmospheric pressure (kPa)
Pr	Prandtl number
q_{Conv}	Net heat flux on test foil (W/m²)
q_j	Supplied heat flux to test foil (W/m²)
q_{loss}	Heat loss from test foil (W/m²)
r	Radial distance from stagnation point (mm)
a	Semi-major axis (mm)
b	Semi-minor axis (mm)
W	Jet half-width (mm)
R	Gas constant
Re	Reynolds number
t_o	Thickness of orifice plate (mm)

Abbreviations

BMO	Bell-mouth orifice
BL	Boundary layer
circ	Circular orifice
CJ	Continuous jet
EF	Enhancement factor
FS	Full scale
HWA	Hot wire anemometry
IR	Infrared
mP	Minor-axis plane
MP	Major-axis plane
PIV	Particle image velocimetry
PSD	Power spectral density
PT	Pressure transducer
SEO	Sharp-edged orifice
SJ	Synthetic jet
TI	Turbulence intensity
TM	Thermal management
ZNMF	Zero-net-mass-flux

Chapter 1

Introduction

1.1 Background

The continuous miniaturization and increasing performance demand of modern electronic devices have led to significant challenges in heat dissipation. As processors and power components become more compact and powerful, they generate intense heat within limited physical spaces. Efficient thermal management has therefore become critical to ensure stable operation, prevent overheating, and extend the lifespan of electronic systems.

Conventional cooling techniques—such as passive heat sinks, forced air convection, and liquid-based cooling—are often constrained by their physical size, complexity, or energy requirements. These limitations become particularly prominent in portable or space-limited applications where bulky cooling systems are impractical.

In recent years, synthetic jets have gained attention as a novel and effective method for localized cooling. Operating through the periodic motion of a diaphragm, synthetic jets produce a pulsed jet of fluid by alternately drawing in and expelling air through a small orifice. Despite having no net mass flow, these jets carry significant momentum and are capable of disturbing boundary layers, thereby enhancing convective heat transfer. Their compact design, low power consumption, and lack of external fluid requirements make them ideal candidates for next-generation cooling solutions.

The performance of synthetic jets is influenced by factors such as actuation frequency, orifice geometry, and spacing between the jet and the heated surface. Among these, the orifice shape and aspect ratio are particularly important in shaping jet structure, flow behaviour, and heat transfer effectiveness.

This thesis focuses on experimentally investigating how elliptical orifices with different aspect ratios affect the cooling performance of synthetic jets. By evaluating thermal behaviour under

controlled laboratory conditions, the study aims to contribute toward optimized design strategies for thermal management in compact electronic systems.

1.2 Classification of Cooling Technologies

Efficient cooling plays a crucial role in the safe and reliable operation of modern electronic and thermal systems. As devices become smaller and more powerful, the challenge of removing excess heat within compact spaces has led to the development of various thermal management methods. These cooling techniques can be broadly classified into three categories based on their mechanism and complexity: Conventional, Advanced, and Hybrid technologies.

Each category offers unique advantages and is selected based on application-specific requirements such as available space, heat load, power consumption, and system reliability.

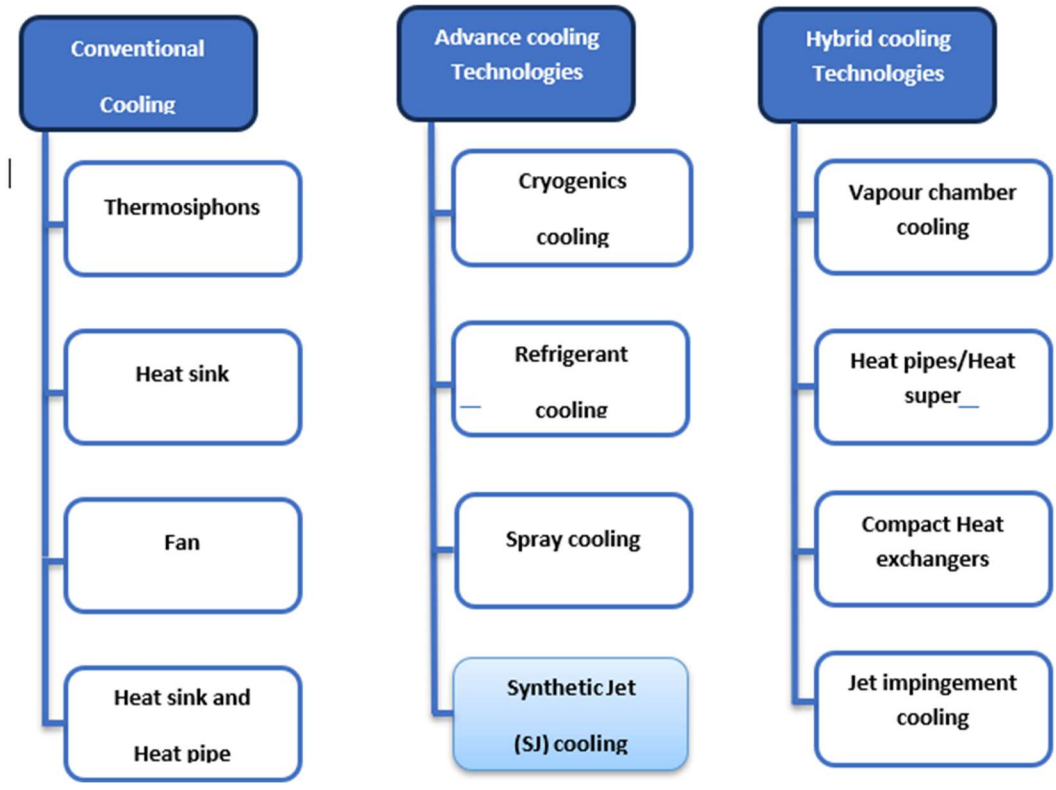

Fig.1.1 Various cooling technologies for thermal management of electronics

1.3 Synthetic Jets

Synthetic jets (SJs) are an innovative class of fluidic devices designed to enhance convective heat transfer by generating pulsating fluid motion from ambient surroundings. Unlike traditional cooling methods that rely on continuous fluid flow or mechanical fans, synthetic jets operate on the principle of zero-net mass flux (ZNMF), meaning there is no net movement of fluid into or out of the system over time.

A synthetic jet is typically formed by an actuator with a vibrating diaphragm and a small orifice or slot. During one half of the actuation cycle, the diaphragm moves outward, drawing fluid into the cavity (ingestion stroke). In the second half of the cycle, the diaphragm moves inward, forcing the fluid out through the orifice (expulsion stroke). This alternating motion produces a series of vortex rings that propagate away from the orifice, generating a jet without requiring any external fluid supply.

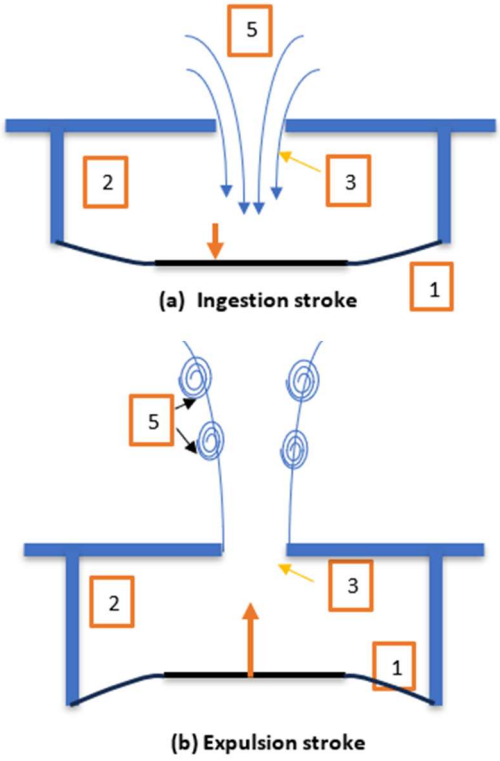

1 Oscillating diaphragm
2 Depth cavity
3 Orifice
4 Ingested fluid
5 Vortices rings

Fig. 1.2 Schematic of synthetic jet during

Key Features of Synthetic Jets

- Compact and Lightweight: Ideal for integration into space-constrained systems.
- Low Power Consumption: Operates using small voltage inputs and efficient actuators.
- No External Fluid Supply Needed: Ingests and expels the same ambient fluid.
- Enhanced Local Cooling: High momentum jets effectively disturb boundary layers, increasing heat transfer rates.
- Flexible Design: Orifice geometry, frequency, and amplitude can be tuned for specific applications.

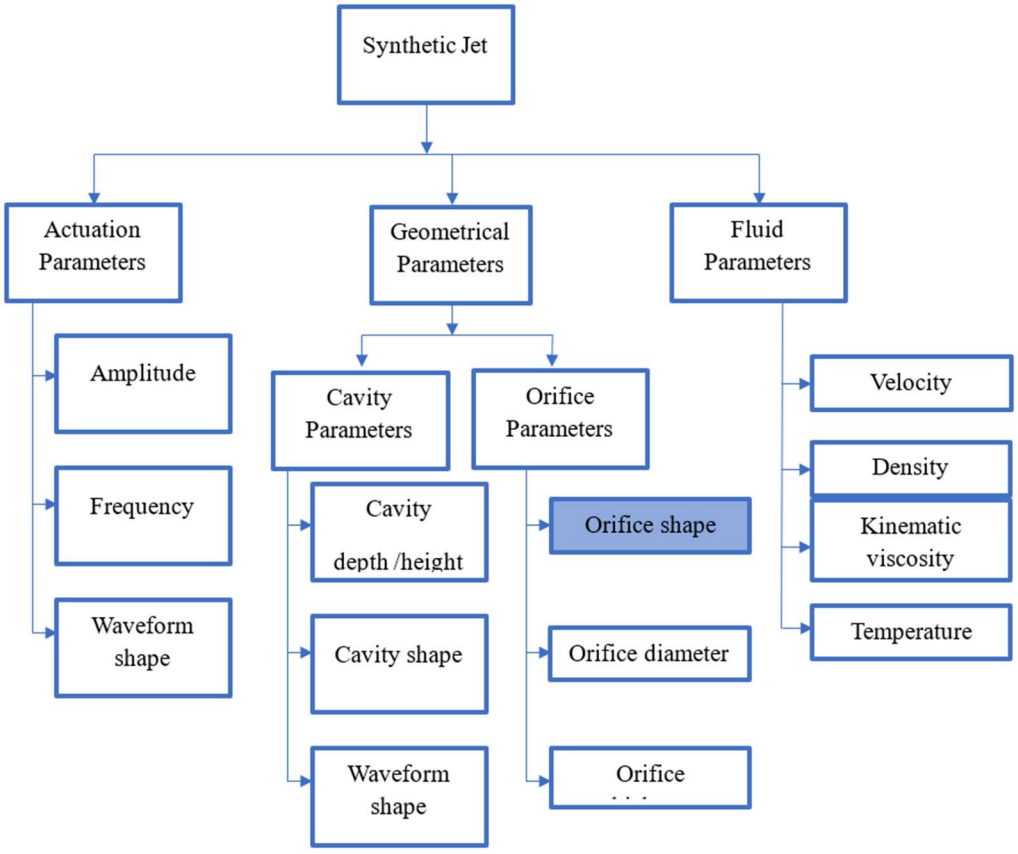

Fig.1.3 Parameters that affect SJ performance

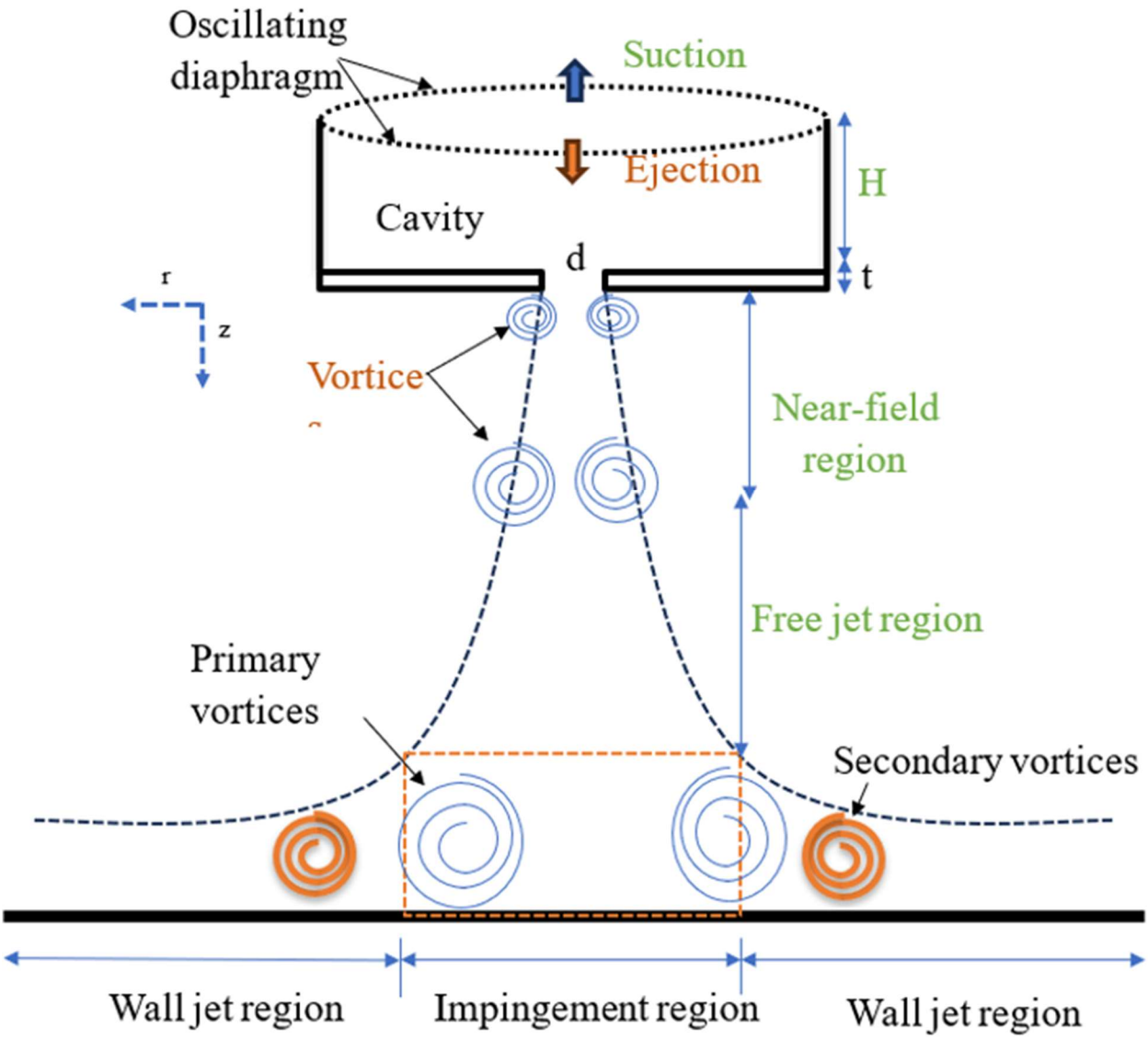

Fig.1.4 Schematic evolution of the synthetic jet flow with different region

1.4 Motivation

The rapid growth in the performance and miniaturization of electronic devices has led to an exponential increase in power density, making thermal management a critical design challenge. Traditional cooling techniques, such as heat sinks, fans, and liquid cooling, often become ineffective or impractical in compact or confined environments. These methods also introduce drawbacks such as added bulk, noise, higher power consumption, or mechanical complexity.

This growing need for efficient, compact, and reliable cooling solutions motivated the exploration of synthetic jet technology, which presents a promising alternative. Synthetic jets are unique in their ability to enhance heat transfer without requiring any external fluid source. They achieve this by creating pulsed jets from ambient air using a simple oscillating diaphragm mechanism.

The compact structure, low energy requirement, and flexibility in design make synthetic jets particularly suitable for applications in microelectronics, embedded systems, and high-performance processors, where space and efficiency are both at a premium.

Furthermore, while existing studies have explored synthetic jets with circular or rectangular orifices, limited work has been done on the effects of elliptical orifice geometry and high aspect ratios. Understanding how these geometries influence flow dynamics and heat transfer performance can provide valuable insights for developing next-generation cooling systems.

Therefore, this project was undertaken to experimentally investigate the cooling performance of synthetic jets with elliptical orifices of varying aspect ratios, aiming to identify optimal configurations for enhanced thermal management in modern electronic applications.

1.5 Objectives of the Project

The primary aim of this research is to investigate the thermal performance of synthetic jets (SJs) using elliptical-shaped orifices with varying aspect ratios. The study is designed to understand how geometric modifications influence heat transfer characteristics during jet impingement cooling. The specific objectives of the project are:

1. **To design and develop an experimental setup** capable of generating synthetic jets using an electromagnetic actuator and measuring surface temperature distributions using thermal imaging techniques.
2. **To examine the cooling performance of synthetic jets** formed through elliptical orifices with different aspect ratios (AR = 1, 2, 6, 10, and 14) under controlled jet-to-surface spacing conditions.
3. **To identify the optimal orifice configuration** that offers the best balance between localized heat transfer intensity and spatial coverage.
4. **To generate heat transfer data and flow observations** that can contribute to the design of efficient, compact, and low-power cooling systems for electronics and thermal management applications.

1.6 Application of Synthetic Jet

Synthetic jets have found diverse applications across several engineering domains due to their compact design, low power consumption, and ability to enhance convective heat transfer without requiring external fluid sources. In electronics cooling, they are used to dissipate heat from compact devices such as CPUs, GPUs, and power modules in laptops, mobile hardware, and high-performance servers. Their integration into LED lighting systems also improves heat management while maintaining silent and compact operation. In aerospace and avionics, synthetic jets serve as effective cooling solutions for sensors and control electronics where space and weight are limited. They are increasingly used in flow control applications, such as delaying boundary layer separation on aircraft wings and turbine blades, thereby improving aerodynamic performance. In biomedical devices and wearable technologies, synthetic jets ensure thermal regulation of sensitive components in confined spaces. Additionally, they play a role in microfluidic systems and lab-on-chip platforms, enabling precise thermal control and fluid manipulation. In high-density

environments like data centers and telecom enclosures, synthetic jets are being explored as localized cooling solutions to reduce dependence on large-scale HVAC systems. Owing to their versatility, synthetic jets are becoming integral to modern thermal management and fluid control strategies in both industrial and consumer applications.

Chapter 2

Literature Review

2.1 Overview

Synthetic jets, also known as zero-net-mass-flux jets, have emerged as a promising method for thermal management and active flow control due to their ability to enhance heat transfer without requiring an external fluid source. Various studies have been conducted to investigate the dynamics, formation, and effectiveness of synthetic jets under different operating and geometric conditions.

Smith and Glezer (1998) pioneered the detailed understanding of synthetic jet actuators, highlighting their ability to produce coherent structures that can interact with boundary layers effectively. They explained the vortex ring formation mechanism during the suction and blowing cycle, which plays a vital role in enhancing heat and mass transfer.

Holman et al. (2005) extended this understanding to the domain of heat transfer by experimentally analysing the impact of synthetic jets impinging on heated surfaces. Their work showed a clear dependency of Nusselt number distribution on orifice geometry and spacing, emphasizing the influence of vortex strength and jet interaction on thermal performance.

Mittal et al. (2008) contributed significantly to the numerical modelling of synthetic jets. Their computational studies captured the development of vortical structures and jet evolution in a synthetic jet actuator, providing insights into how flow unsteadiness and actuator frequency affect boundary layer interactions.

Pavlova and Amitay (2006) investigated the application of synthetic jets in electronics cooling. They found that the non-intrusive and localized nature of these actuators made them well-suited for applications where traditional cooling methods fall short. Their results indicated a considerable improvement in heat transfer performance, especially in regions with high thermal loads.

Shuja et al. (2007) focused on the role of orifice shape in the performance of synthetic jets. They compared circular and rectangular orifices and observed that rectangular nozzles offer a broader

area of influence and more efficient cooling, which is beneficial in electronics and localized heat dissipation.

Guo et al. (2012) examined the cooling performance of synthetic jets in pulsed mode and found enhanced convective heat transfer due to improved mixing and entrainment. The study highlighted that pulsed synthetic jets could be more energy-efficient while delivering superior performance compared to steady-state systems.

Chatterjee et al. (2020) reviewed the application of synthetic jets in miniature devices and microscale systems. Their review stressed the importance of geometric optimization and highlighted the need for further research in waveform control, jet directionality, and multi-orifice systems to enhance performance.

Together, these studies provide a comprehensive foundation for the present work, which aims to experimentally and numerically investigate the performance of synthetic jets with varying orifice geometries and excitation waveforms. These parameters have been shown to significantly impact the thermal and flow behaviour of the jets and thus hold the key to optimizing synthetic jet design for advanced thermal management systems.

2.2 Cooling Technologies Overview

Thermal management remains a critical challenge as electronic components continue to scale down while heat flux increases significantly. Conventional cooling methods, including heat sinks, forced convection fans, and heat pipes, provide effective solutions in many scenarios but face limitations in compact and high-power density environments.

To address this, advanced cooling technologies such as spray cooling, phase-change systems, and synthetic jet cooling have emerged. Synthetic jets are especially promising due to their low power consumption, small size, and zero-net-mass-flux operation, making them ideal for local, targeted cooling in electronics.

2.3 Characteristics of Synthetic Jets

Synthetic jets (SJs) are formed by periodic suction and expulsion of ambient fluid through an orifice without a net mass flow. This mechanism generates vortex rings that promote mixing and enhance convective heat transfer. Pioneering work by Smith and Glezer (1998) established the effectiveness of SJs in disrupting boundary layers and improving cooling efficiency.

Straccia and Farnsworth (2021) experimentally demonstrated that vortex ring dynamics, particularly axis-switching behaviour, is a dominant mechanism in non-circular synthetic jets, with significant implications for entrainment and heat transfer performance. Their results indicated that higher aspect ratios (ARs) increased lateral deformation and entrainment through stronger vortex ring bifurcations and switching.

2.3.1 Axis Switching Phenomenon

This phenomenon refers to periodic interchange of major and minor axes in a non-circular jet as it evolves downstream. This effect occurs due to self-induced velocity variations, caused by vortex interactions in the jet. In synthetic jets, where fluid is periodically expelled and entrained without net mass flow, axis switching plays a critical role in determining the mixing, entrainment, and cooling efficiency.

2.4 Gaps Identified in Literature

From the reviewed studies, it is evident that synthetic jets are highly effective for localized heat transfer enhancement, particularly when using non-circular orifices. However, the role of elliptical geometries and their aspect ratio on the performance of synthetic jet cooling systems remains insufficiently addressed. This thesis aims to bridge this gap through a detailed experimental investigation using elliptical orifices with varying ARs, thermal imaging, and controlled jet-to-surface spacing to assess heat transfer improvements; some of the key issues are highlighted below.

- Limited experimental studies exist on elliptical orifices, particularly with high aspect ratios (AR > 5).
- The impact of AR on vortex bifurcation, axis-switching location, and entrainment rate is underexplored, especially under low jet-to-surface spacing conditions relevant for compact cooling.
- Prior studies have focused more on flow visualization and less on thermal performance data using tools like thermal imaging.
- Comparative analysis of heat transfer enhancement across various ARs under identical actuation conditions is scarce

Chapter 3

Experimental Methodology

3.1 Overview

This chapter details the experimental approach used to investigate the cooling performance of synthetic jets (SJs) formed through elliptical orifices with varying aspect ratios (AR = 1, 2, 6, 10, 14). The primary objective was to evaluate the heat transfer behaviour of these jets during impingement cooling on a heated surface using a thermal imaging camera. The methodology includes a description of the test facility, orifice configurations, instrumentation, and the data acquisition and processing techniques employed.

3.2 Experimental Setup

The experimental test facility was developed to generate synthetic jets using an electromagnetic actuator and assess their thermal impact on a target surface. The major components of the setup are described below:

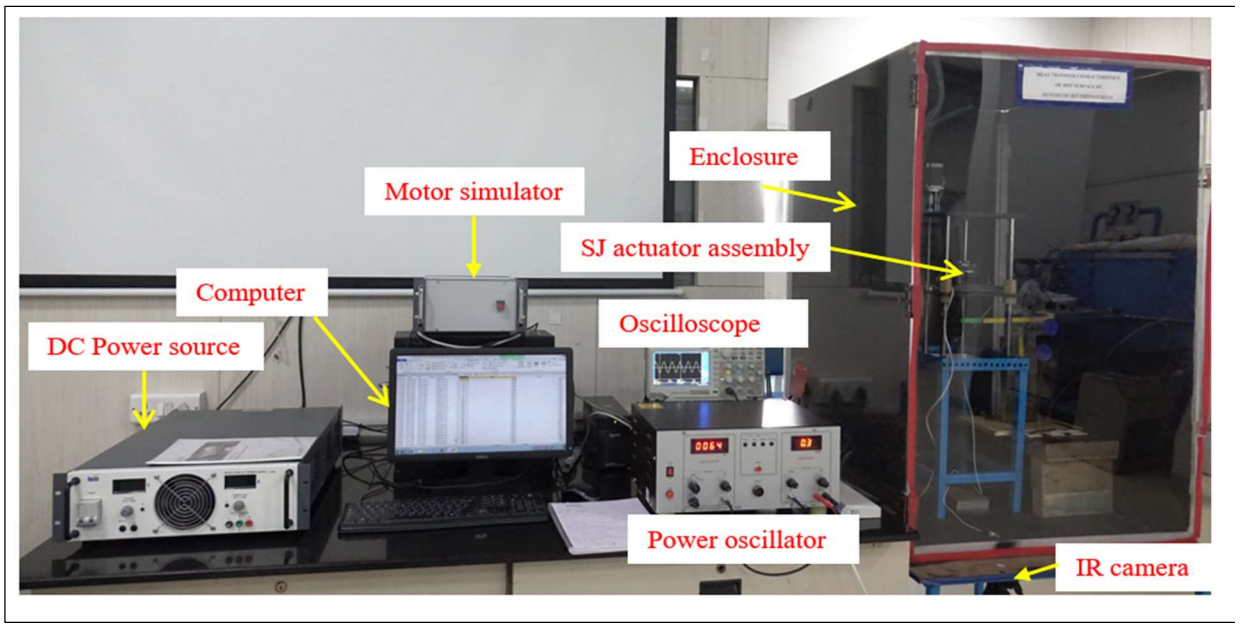

Fig.3.1 Experimental Set-up

3.2.1 Synthetic Jet Actuator

The actuator consists of a cylindrical cavity enclosed by a vibrating diaphragm. It is excited by a power oscillator driven by a DC power supply, which generates a sinusoidal signal to control the diaphragm motion. The periodic movement of the diaphragm induces suction and expulsion strokes, forming the synthetic jet through an orifice plate mounted at the cavity exit.

3.2.2 Orifice Plates

Removable orifice plates with elliptical openings were fabricated to test different aspect ratios i.e. AR = 1, 2, 6, 10, and 14

Each orifice was laser-cut from an acrylic sheet, keeping consistent orifice area across all aspect ratios to isolate the influence of shape on jet behaviour.

Parameters	**Operating range**
Orifice shapes	Elliptical
Orifice plate thickness, (t)	5 mm
Orifice equivalent diameter, (d)	15 mm
Actuation frequency	40 Hz
axial surface spacings, (z/d)	1-16
cavity depth, (h)	26 mm
diaphragm diameter (D)	133.35 mm

Table.1.1 Variable geometric and operational parameters used in the current study.

Orifice	Semi-major axis (r_1) (mm)	Semi-minor axis (r_2) (mm)	Aspect ratio ($AR = \frac{r_1}{r_2}$)	Total Equivalent area (mm^2)
Circular	7.5	7.5	1	176.71
Elliptical	7.98	3.99	2	176.67
Elliptical	15	3.75	4	176.67
Elliptical	18.36	3.06	6	176.65
Elliptical	23.72	2.37	10	176.65
Elliptical	28	2	14	176.67

Table.1.2 Design parameters of different elliptical aspect ratio orifice

3.2.3 Orifice Design and Aspect Ratio Details

Aspect Ratio (AR)- is the ratio of the major axis (longest dimension) to minor axis (shortest dimension) of a noncircular jet or nozzle.

$$AR = \frac{MAJOR\ AXIS\ LENGTH}{MINOR\ AXIS\ LENGTH}$$

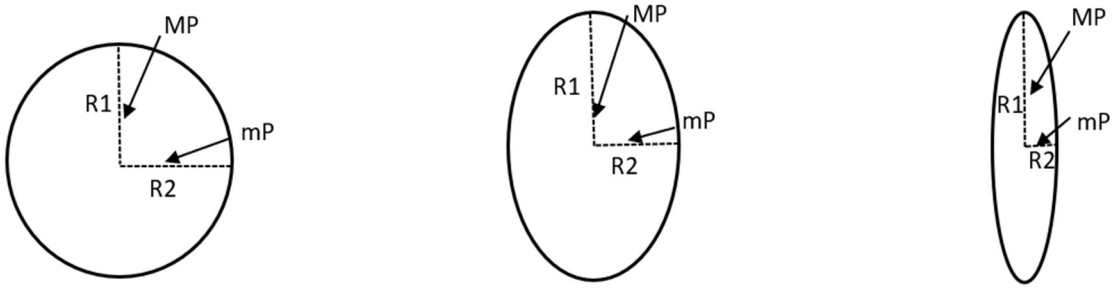

Fig.3.2 Schematic view of different elliptical shaped orifices

3.2.4 Test Surface

A stainless-steel plate (AISI-304) was used as the impingement surface. It was uniformly heated using a resistive heating element mounted underneath the plate. The surface finish was controlled to minimize radiation losses and ensure accurate temperature readings.

Material of test surface	AISI-304
Area(A),mm^2	120*120
Thickness, mm	0.05
Density (ρ)Kg/m^3	7930
Specific heat capacity (C_P) J/KgK	500
Thermal conductivity(k)	16.2

Table.1.3 Dimension of thermo-physical properties of test surface

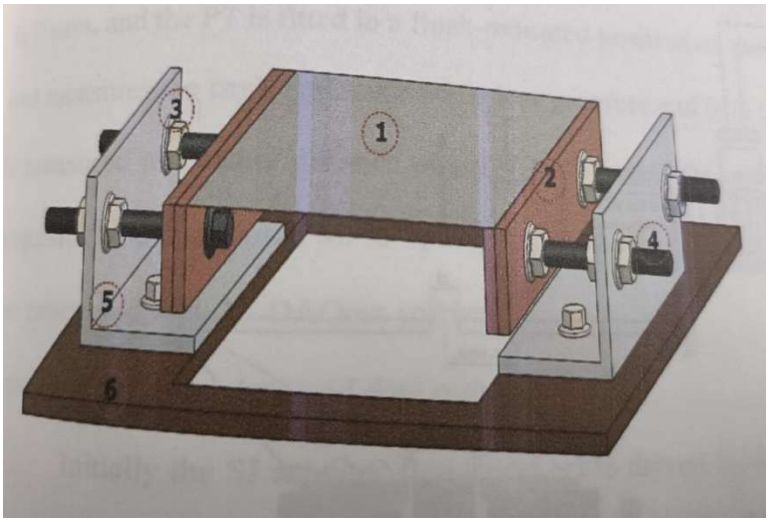

1-Heating foil

2-Cu-bus bars

3-Fasteners

4-Tightening bolt

5-L-shaped support (MS)

6-Bakellite plate

Fig.3.3 Schematic of heating plate assembly used for heat transfer study in present investigation.

3.2.5 Traversing Mechanism

A precision traversing mechanism was integrated into the setup to adjust the jet-to-surface spacing (z/d). This allowed controlled variation in the vertical distance between the orifice and the test surface during experiments.

3.3 Measurement and Instrumentation

3.3.1 Temperature Measurement

Surface temperature distribution was recorded using a FLIR A65SC infrared thermal imaging camera, which offers high spatial and thermal resolution. The camera was calibrated before each test to account for emissivity and ambient radiation.

3.3.2 Data Acquisition System

- **Power Supply**: DC power source (0–30 V, 5 A) for the actuator
- **Function Generator**: To set the excitation frequency of the diaphragm.
- **Multimeter/Thermocouple**: For reference temperature verification and heater control

All data were recorded after thermal equilibrium was reached on the test surface.

3.4 Test Conditions

- **Jet-to-surface spacings (z/d)**: 1, 3, 6, and 1
- **Excitation frequency**: Fixed at diaphragm resonance frequency (~40 Hz)
- **Input voltage**: Set to ensure stable diaphragm motion without overloading.
- **Ambient conditions**: Room temperature (25–34°C), low airflow environment

3.5 Data Processing and Calculations

3.5.1 Heat Transfer Coefficient

The local heat transfer coefficient (h_i) and its equivalent Nusselt number (Nu_i) for i^{th} control volume in SJ cooling can be figured out as:

$$h_i = \frac{q_{conv,i}}{A_i(T_{s,i} - T_{a,i})} \; and \; Nu_i = \frac{h_i d}{k_f} \tag{3.1}$$

Here, . T_S and T_a designated the heated test foul temperature and the ambient temperature respectively, while q_{conv} denotes the net heat flux available to the test surface after considering the heat loss.

$$q_{conv,i} = q_{j,i} - q_{loss,i} = q_{j,i} - \left(q_{conv,b(i)} + q_{rad,b(i)} + q_{rad,t(i)}\right) \tag{3.2}$$

Here, q_i implies the supplied heat flux across the test foil based on joule heating. By measuring the voltage drop (V) across the test foil and flowing current (I), heat supplied to test foil (q_i) can be estimated. However, q_{loss} signifies the total heat loss (majorly by natural convection and radiation, which can be calculated as given below.

$$q_{conv,i} = \left(\frac{\mathrm{V}\times I}{A_S}\right) A_i - [(h_{e_{ff},b} A_i\left(T_{S,i} - T_{a,i}\right) + \sigma \varepsilon_t A_i (T_{s,\mathrm{i}}^4 - T_{a,\mathrm{i}}^4)] \tag{3.3}$$

The heat loss ($q_{loss,b}$) from the back surface of test foul depends on the difference in temperature of heated surface test foil (T_S) and ambience (Ta). The heat loss calculation on thin foil when the jet is in off mode. In this calculation, a known electrical power in terms of voltage (V) and current (I) is supplied to the test surface temperature is recorded while the front side of the foil (i.e. impinging surface) is well insulated with glass wool. Based on the temperature difference ($T_s - T_a$) and the corresponding electrical power supplied, a linear curve fitting provides a correlation for the heat loss form the test surface. The heat loss curve is presented in terms of the temperature difference between target surface and ambient condition as shown in fig. The obtained correlation for the heat loss is as below:

$$Q_{loss,b} = 0.23143 \times (T_s - T_a) - 0.31364 \quad (3.4)$$

$$h_{eff,b} = 16.068 - \frac{21.78}{(T_s - T_a)} \quad (3.5)$$

Further effective heat transfer coefficient () for the heat loss from the back surface (surface opposite to jet impingement) is computed which accounts both the natural and convective and radiative heat transfer from the back surface. The maximum effective heat transfer coefficient for the back surface due to natural convection and radiative heat transfer is found to be 16.07 $W|m^2k$ .Also, the radiative heat loss from the front side of targeting surface () is obtained. which accounts to be a maximum 2.1% of the total heat supplied. The total heat loss computed to be maximum of 21.1% of the heat supplied at $(T_s - T_a = 25℃)$ accounts majorly due to natural convective and radiative heat loss from back surface of the impinging foil.

The calculations for quantifying the average heat transfer coefficient (h_{avg}) and average Nusselt number (Nu_{avg}) is as follows.

$$h_{avg} = \frac{\Sigma q_{Conv,i}}{\Sigma A_i (T_{s,i} - T_{a,i})} and\ Nu_{avg} = \frac{h_{avg} d}{k_f} \quad (3.5)$$

Where k_f denotes the thermal conductivity of working fluid, In the present experimentation, the area averaged Nu (Nu_{avg}) is computed by calculating Nu at each pixels of the IR image of the cooling surface, The IR temperature matrix of the considered surface is processed with a MATLAB code to evaluate an average heat transfer rate by providing input parameters of heat flux (q_{conv}) and ambience temperature (T_α).

Chapter 4

Results and Discussion

4.1 Effect of Jet-to-Surface Distance (z/d)

This chapter presents the experimental findings on the cooling performance of synthetic jets (SJs) impinging through elliptical orifices with various aspect ratios (AR = 1, 2, 6, 10, 14) at different jet-to-surface distances (z/d = 1, 3, 6, and 14). The results are discussed in terms of temperature distribution, local and average Nusselt number variations, and the influence of orifice geometry on flow behaviour. These insights help identify the optimal conditions for maximizing convective heat transfer in compact cooling applications.

4.1.1 Heat Transfer Performance at z/d = 1

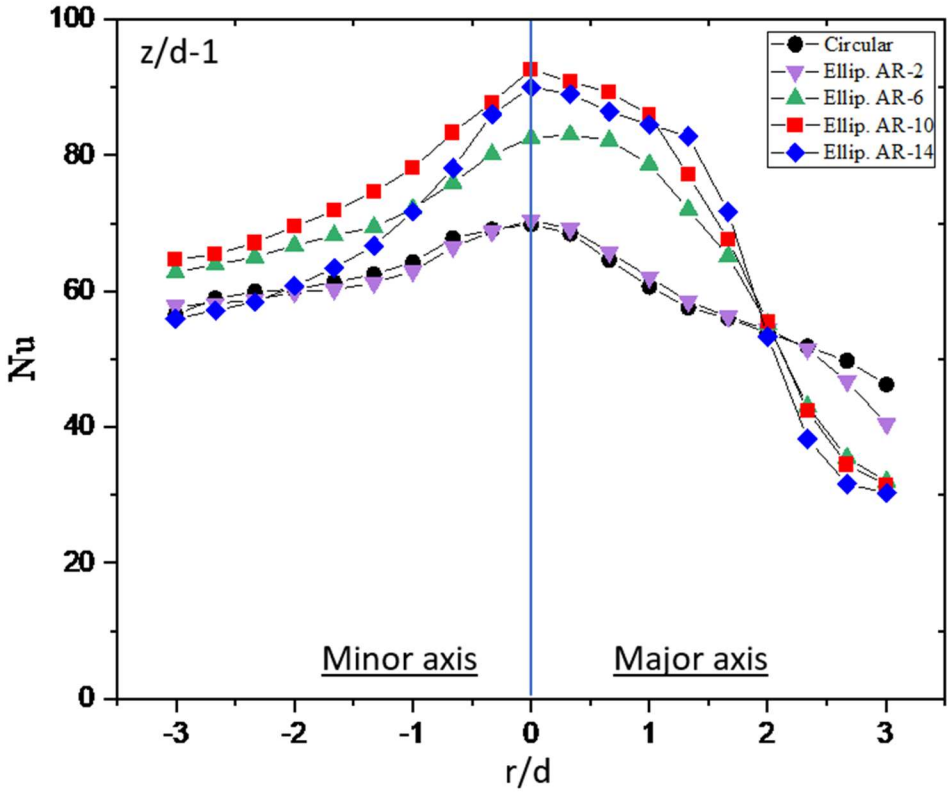

Fig.4.1 Nusselt Number vs Radial Location at z/d = 1

The peak Nusselt number is consistently observed at the stagnation point (r/d = 0) across all tested configurations, indicating the highest heat transfer directly beneath the impinging jet. As the aspect ratio increases, particularly for AR = 10 and 14, the heat transfer footprint becomes significantly broader, demonstrating enhanced lateral coverage. Among these, AR = 10 stands out by combining a relatively high peak Nusselt number with an extended radial distribution. This suggests that the jet remains more coherent and retains higher momentum near the surface, resulting in strong impingement. The elliptical geometry of higher AR jets facilitates improved entrainment and lateral momentum spreading, especially at low z/d values, where the flow remains close to the target surface. Overall, AR = 10 provides the best compromise between peak heat transfer intensity and spatial uniformity, making it the most effective configuration for impingement cooling under these conditions.

4.1.2 Heat Transfer Performance at z/d = 3

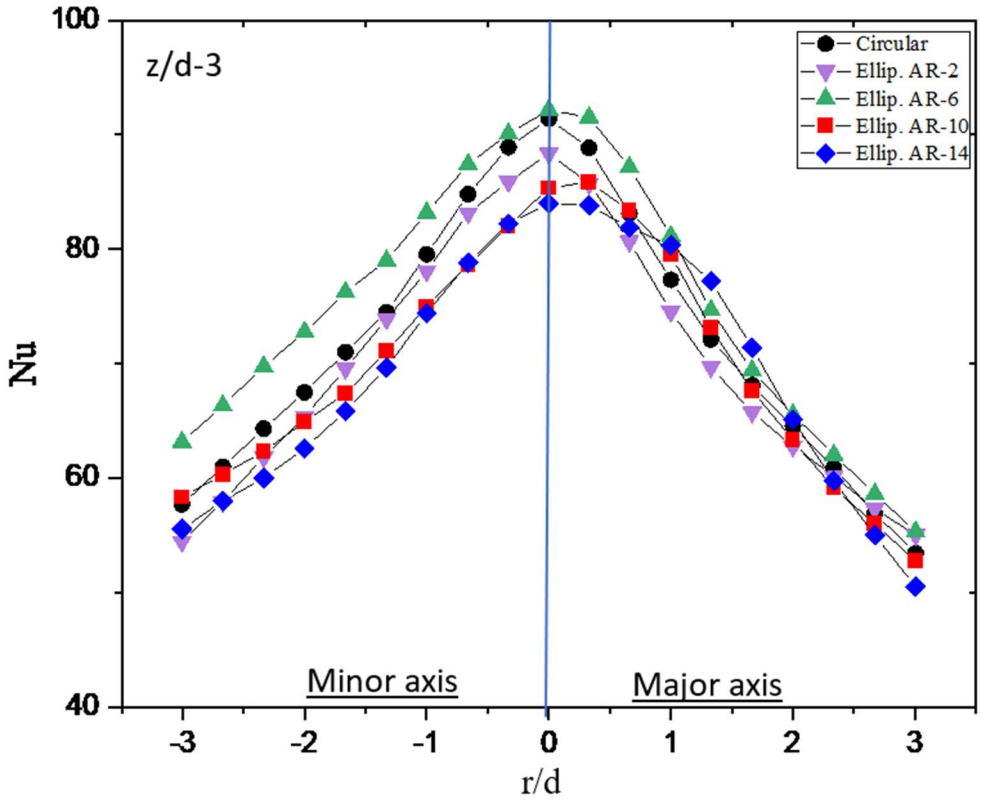

Fig.4.2 Nusselt Number vs Radial Location at z/d = 3

At z/d = 3, the peak Nusselt numbers decrease slightly for all jet configurations compared to the closer spacing at z/d = 1, indicating the effect of increased diffusion with distance. Despite this reduction, elliptical jets—particularly those with AR = 10 and 14—maintain a wider and flatter heat transfer profile, showcasing their ability to distribute thermal energy more uniformly across the surface. In contrast, the circular orifice (AR = 1) exhibits a noticeable drop in performance beyond the central region, with a steep decline in Nusselt number as r/d increases. This behavior suggests that while jet diffusion becomes more pronounced at this spacing, higher aspect ratio elliptical jets are more effective in sustaining thermal footprints. Their geometry supports stronger, more resilient vortex structures that help preserve entrainment and flow coherence. Among all, AR = 10 continues to demonstrate the best combination of uniformity and average heat transfer, affirming its effectiveness even as the impingement distance increases.

4.1.3 Heat Transfer Performance at z/d = 6

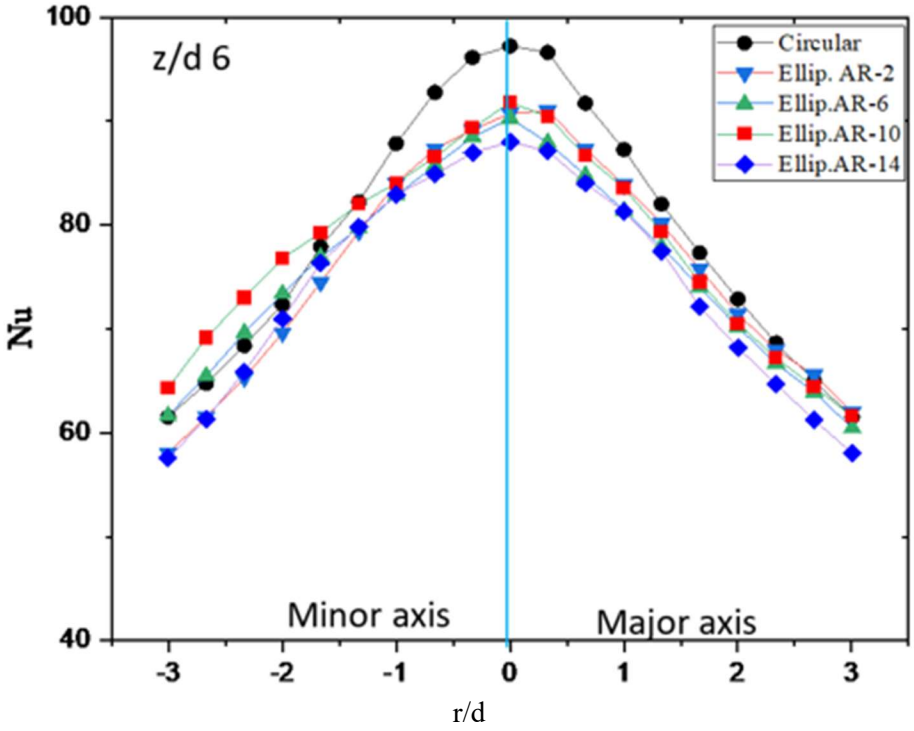

Fig.4.3 Nusselt Number vs Radial Location at z/d = 6

At a jet-to-surface spacing of z/d = 6, the peak Nusselt values are significantly reduced for all aspect ratios, reflecting the weakening of the jet's impingement intensity due to increased diffusion. Nevertheless, the thermal footprint continues to expand laterally, albeit with diminished intensity. Among the tested configurations, AR = 14 demonstrates better performance in the outer radial regions, while AR = 10 offers a more balanced distribution between central intensity and peripheral coverage. The observed reduction in peak heat transfer is attributed to a loss of jet coherence over the extended distance, which particularly impacts the stagnation zone. However, in high aspect ratio jets, the formation of secondary vortices helps sustain heat transfer in the outer zones. AR = 10 thus emerges as the most effective compromise, maintaining sufficient intensity at the center while ensuring a reasonably wide thermal spread, making it ideal for applications requiring both focused and distributed cooling.

4.1.4 Heat Transfer Performance at z/d = 10

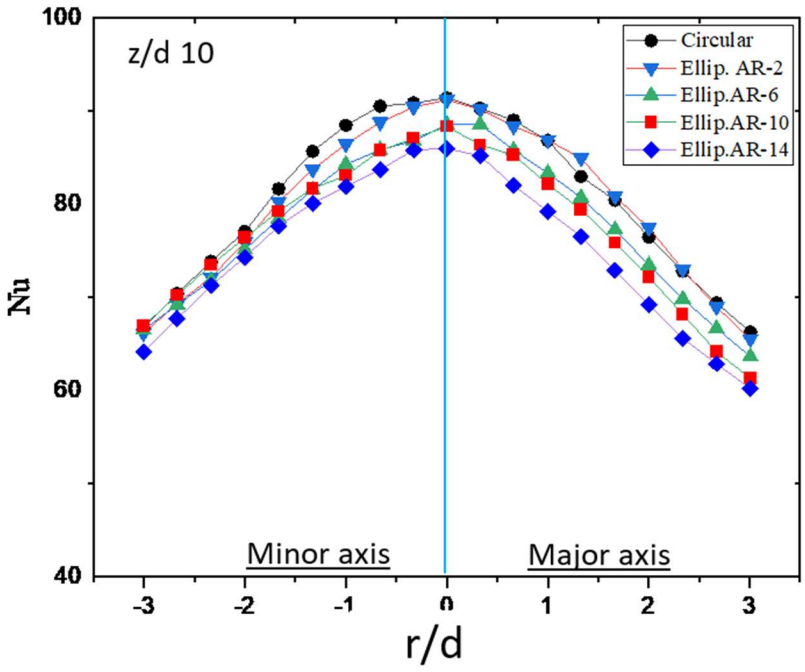

Fig.4.4 Nusselt Number vs Radial Location at z/d = 10

At a jet-to-surface spacing of z/d = 10, all synthetic jet configurations exhibit significantly diffused performance, indicating substantial momentum loss before the jet reaches the impingement surface. Despite this overall reduction, elliptical jets with AR = 10 and 14 continue to deliver higher heat transfer rates compared to the circular jet (AR = 1), which becomes the least effective across all radial positions. The performance degradation at this larger spacing is primarily due to the diminished coherence of the jet flow, where diffusion overtakes directed momentum. However, elliptical jets still maintain relative superiority owing to their ability to promote enhanced entrainment and generate secondary vortex structures that contribute to peripheral mixing and thermal transport. Notably, while AR = 14 shows strong outer-region performance, the marginal gain over AR = 10 is minimal, suggesting diminishing returns at excessively high aspect ratios. Therefore, AR = 10 appears to offer the most balanced and efficient configuration, even under highly diffusive conditions.

4.1.5 Heat transfer performance along both the major and minor axes of the elliptical synthetic jet at various z/d ratios and aspect ratios (AR).

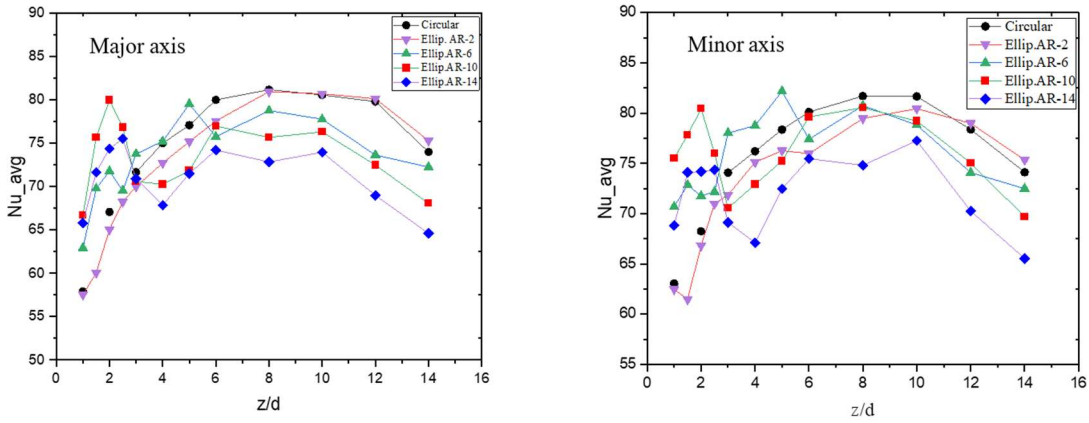

Fig.4.5: Variation of Nusselt number along (a) major axis and (b) minor axis for different orifice aspect ratios (AR = 1–14).

Flow Behaviour Along the Major Axis

Along the major axis, the elliptical orifices direct the synthetic jet in a broader, laterally stretched form. The contour plots clearly show that, as the aspect ratio increases, the flow becomes progressively elongated and more spread out along this axis. For instance, with AR = 1 (circular), the flow maintains symmetry and has a compact structure. However, with AR = 6, and more prominently with AR = 10 and 14, the jet core is observed to extend further downstream, while the vortex structures stretch outward, indicating strong entrainment and mixing in the lateral direction.

The presence of elongated vortices along the major axis supports broader interaction with the ambient fluid, which enhances convective heat transfer over a larger surface area. This effect is most pronounced in the AR = 10 case, where the contour lines indicate a balanced combination of axial jet penetration and radial spread. The flow remains coherent enough to deliver energy to the stagnation region but diffuses effectively to cover a wider zone.

This behaviour implies that higher aspect ratio elliptical jets are particularly well-suited for applications requiring uniform surface cooling across extended domains. The results along the major axis thus emphasize the value of geometric shaping of the orifice to manipulate flow structure and thermal coverage.

Flow Behaviour Along the Minor Axis

In contrast, the minor axis presents a more focused and concentrated jet behaviour. Contour plots along this direction illustrate that, although the jet remains symmetric about the centreline, the spread is significantly reduced compared to the major axis. For AR = 1, the jet expands equally in all directions due to its circular symmetry. However, as the aspect ratio increases, the lateral spread in the minor direction becomes more confined.

Notably, at AR = 10 and 14, the flow along the minor axis appears tightly channelled with a shorter core length and more compact vortex rings. The entrainment from the surroundings is less dominant, and the momentum remains focused in a narrow region near the centre. This results in intensified stagnation zone heat transfer but reduced surface coverage.

The minor axis jets are therefore more effective for localized cooling, such as hotspot treatment in electronics, where high-intensity, narrowly targeted heat removal is desired. While the overall heat transfer area is less, the local Nusselt numbers near the impingement point can be relatively higher due to the jet's focused energy delivery.

Summary

Together, the major and minor axis flow visualizations reveal the anisotropic nature of elliptical synthetic jets. The major axis favors uniform and widespread cooling, while the minor axis supports high-intensity, focused thermal performance. The plots affirm that AR = 10 provides the most balanced behaviour—combining strong central impingement with extended lateral diffusion—making it ideal for applications requiring both reach and intensity.

4.2 Surface Temperature Distribution

The thermal images captured by the FLIR A65SC infrared camera revealed significant differences in temperature patterns across various configurations:

- At z/d = 1, strong stagnation point cooling was observed, with peak heat transfer at the centre.
- As z/d increased to 3 and 6, the cooling footprint became wider, but the intensity of heat transfer decreased.
- At z/d = 10, the effect of impingement weakened, indicating reduced jet momentum at larger distances.

Elliptical jets with higher ARs (especially AR = 10) showed a broader and more uniform temperature profile, suggesting enhanced lateral mixing and improved vortex dynamics.

4.2.1 Temperature distribution contour

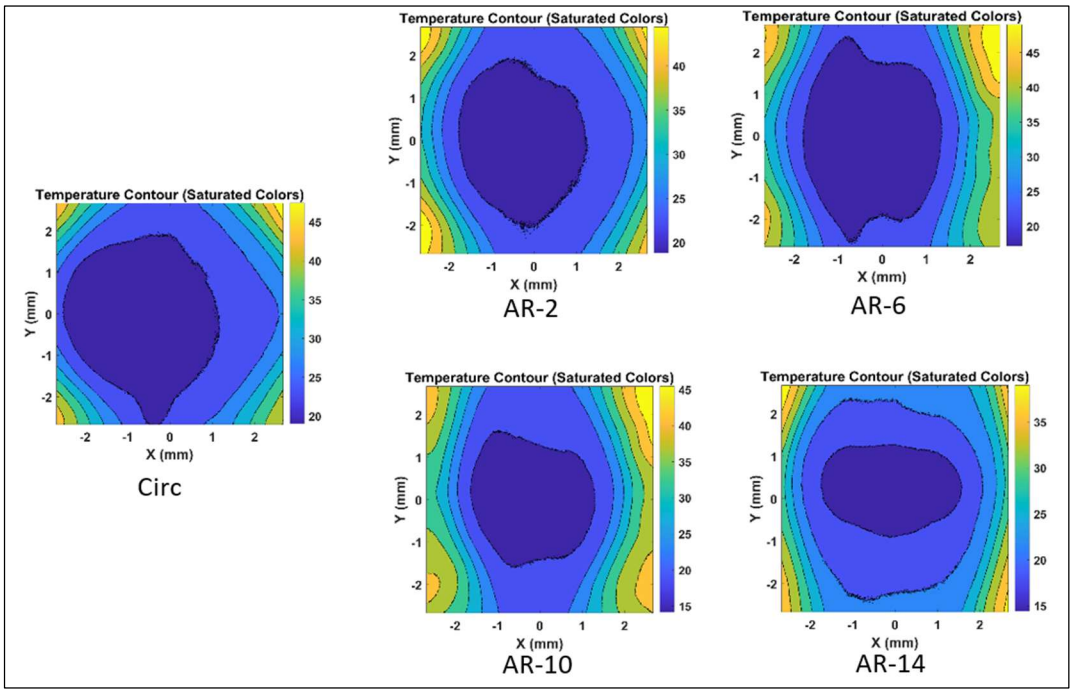

Fig.4.6: Contour map of temperature distribution for different elliptical aspect ratio orifice at dimensionless spacing $\frac{z}{d} = 1$

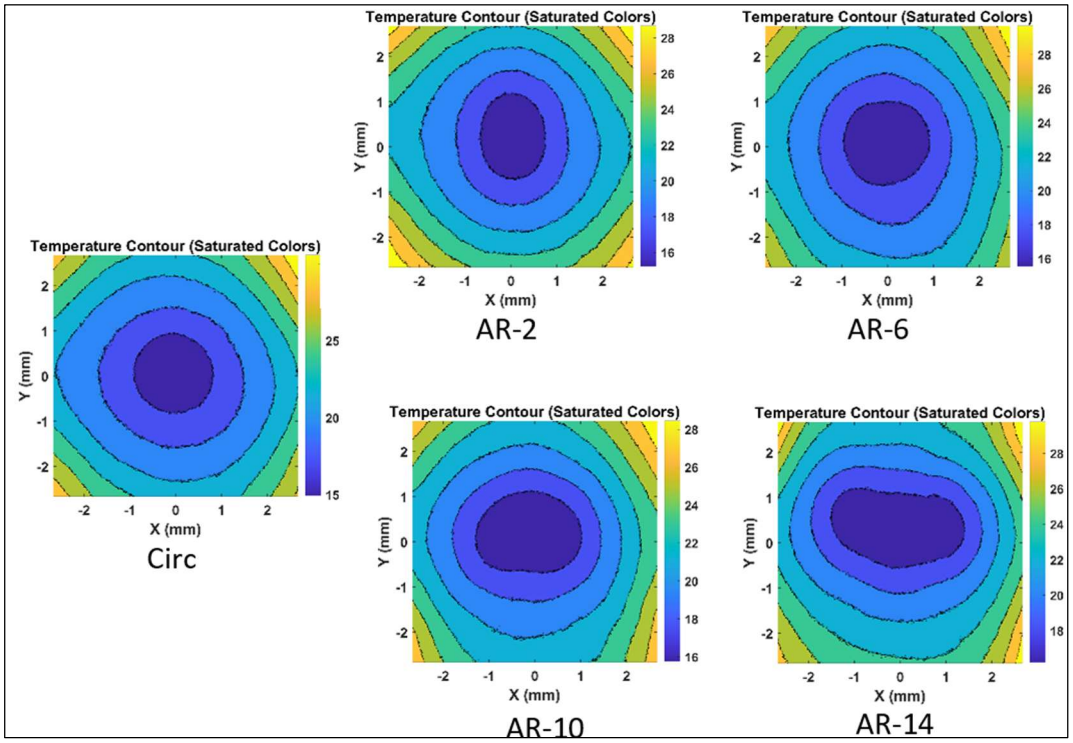

Fig.4.7: Contour map of temperature distribution for different elliptical aspect ratio orifice at dimensionless spacing $\frac{z}{d} = 3$

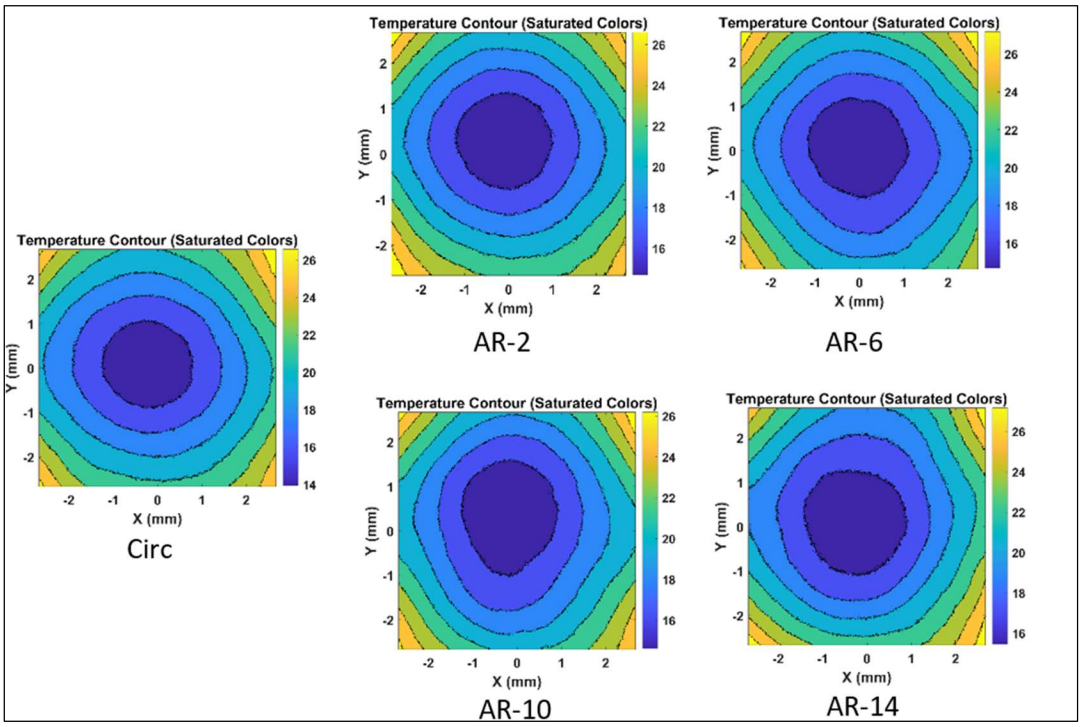

Fig.4.8: Contour map of temperature distribution for different elliptical aspect ratio orifice at dimensionless spacing $\frac{z}{d} = 6$

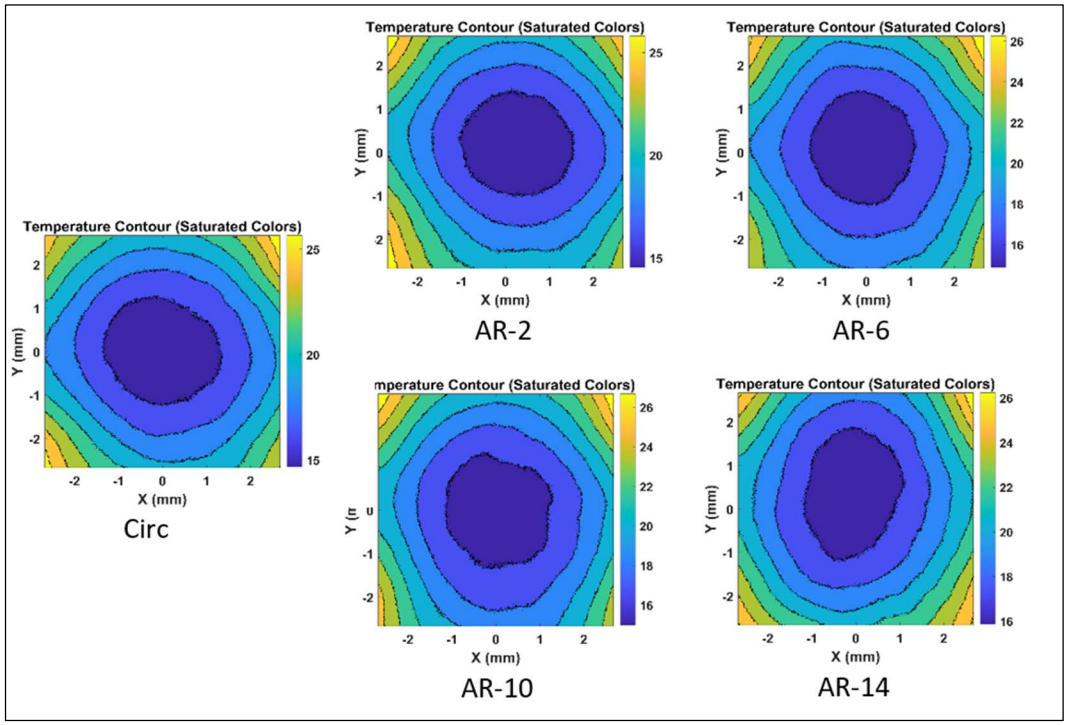

Fig.4.9: Contour map of temperature distribution for different elliptical aspect ratio orifice at dimensionless spacing $\frac{z}{d} = 10$

The contour plots of surface temperature distribution for various elliptical orifice aspect ratios (AR) at different jet-to-surface spacings (z/d = 1, 3, 6, and 10) clearly illustrate the evolution of synthetic jet behavior and its impact on thermal performance. In Fig 4.6 (z/d = 1)**,** jets impinge directly onto the surface, producing highly focused cooling at the stagnation point. The thermal footprint is sharply defined, with peak cooling intensity located at the center. As shown in Fig 4.7 (z/d = 3)**,** the thermal spread increases as the jet begins to diffuse, and while the intensity slightly diminishes, elliptical orifices with higher ARs—particularly AR = 10 and 14—still maintain a broad and uniform temperature distribution. In Fig 4.8 (z/d = 6)**,** the contours show further lateral expansion of the thermal field, with reduced central intensity but sustained peripheral performance, especially for AR = 14. Fig 4.9 (z/d = 10) reflects a significant drop in core jet momentum across all configurations, but elliptical jets retain comparatively better thermal coverage. Notably, across Figures 4.7 to 4.9, signs of the axis switching phenomenon become apparent. In jets with AR ≥ 10, the initially elongated jet structure along the major axis begins to spread into the minor axis direction downstream, resulting in a more symmetrical thermal pattern and enhanced lateral heat transfer. This redistribution of momentum contributes to uniform cooling and a broader effective impingement zone. Overall, the contour plots validate that AR = 10 provides the optimal combination of strong impingement and wide-area cooling, driven by enhanced vortex dynamics and axis switching effects.

4.3 Influence of Aspect Ratio (AR)

Increasing the AR of the elliptical orifice had a pronounced effect on the thermal and flow behaviour of the synthetic jets:

- Low ARs (1–2) produce narrow, concentrated jets with limited lateral spread.
- Intermediate AR (6) is found to balance centreline intensity with broader spreading.
- High AR (10–14) exhibit extended vortex core lengths and better entrainment, improving heat transfer across a wider area.

However, beyond AR = 10, the performance decreases moderately, indicating diminishing returns due to excessive jet elongation and loss of core momentum.

Chapter 5

Conclusion and Future Scope

5.1 Conclusion

This study experimentally investigated the cooling performance of synthetic jets (SJs) generated through elliptical orifices with varying aspect ratios (AR = 1, 2, 6, 10, and 14) under different jet-to-surface spacing conditions (z/d = 1, 3, 6, and 10). The objective was to evaluate the influence of orifice geometry on heat transfer characteristics and identify an optimal configuration for efficient thermal management in compact systems.

The key conclusions drawn from the research are as follows:

- Elliptical synthetic jets significantly enhance local and average heat transfer compared to circular jets, primarily due to improved vortex dynamics and lateral flow spreading.
- Aspect ratio (AR) plays a crucial role in determining jet structure. Jets with AR = 10 provided the best thermal performance, offering the highest average Nusselt numbers across all tested z/d ratios.
- At low jet-to-surface spacings (z/d = 1–3), the cooling effect was most pronounced, with high stagnation-point Nusselt numbers and strong surface impingement.
- Beyond AR = 10, the improvement in heat transfer began to saturate, suggesting diminishing returns for higher aspect ratios.
- Infrared thermal imaging confirmed more uniform and widespread cooling for higher AR elliptical jets, supporting the quantitative heat transfer results.

Overall, the findings validate that elliptical synthetic jets with AR = 10 and low z/d spacing present an optimal design for compact and efficient thermal management in electronics and microsystems.

Although the present study provides important insights into synthetic jet cooling with elliptical orifices, several opportunities exist to extend this work:

1. Numerical Simulations: Conduct detailed CFD simulations to visualize vortex structures, quantify flow fields, and validate experimental heat transfer trends.
2. Transient Analysis: Study the dynamic cooling behaviour of synthetic jets under varying heat loads or pulsed operation.
3. Multi-Jet Configurations: Investigate interactions between multiple synthetic jets in array layouts to assess scalability for larger surface areas.
4. Alternative Actuation Mechanisms: Explore piezoelectric or MEMS-based actuators to reduce power consumption and improve integration in micro-devices.
5. Extended Geometries and Fluids: Analyse other non-circular geometries (e.g., lobed, square) or use different working fluids to study their impact on performance.
6. Real-Time Application Testing: Integrate the SJ cooling system into an actual electronic device (e.g., CPU, LED) and evaluate real-world performance.

The outcomes of this research form a strong foundation for further development of high-efficiency, low-profile cooling solutions using synthetic jet technology.

References

1. M. Jain, B. Puranik, and A. Agrawal, “A numerical investigation of effects of cavity and orifice parameters on the characteristics of a synthetic jet flow,” Sensors and Actuators A: Physical, vol. 165, no. 2, pp. 351–366, 2011.

2. R. Singh and S. P. Singh, “Thermal characteristics of synthetic jets for cooling applications: A comprehensive study,” Renewable and Sustainable Energy Reviews, vol. 103, pp. 602–620, 2019.

3. Y. Zhang, P. Li, and Y. Xie, “Numerical investigation of heat transfer characteristics of impinging synthetic jets with different waveforms,” International Journal of Heat and Mass Transfer, vol. 125, pp. 1017–1027, 2018.

4. G. Krishnan and K. Mohseni, “An experimental study of a radial wall jet formed by the normal impingement of a round synthetic jet,” European Journal of Mechanics - B/Fluids, vol. 29, no. 4, pp. 235–245, 2010.

5. J. C. Straccia and J. A. N. Farnsworth, “Axis switching in low to moderate aspect ratio rectangular orifice synthetic jets,” Physical Review Fluids, vol. 6, no. 5, p. 054702, 2021.

6. T. V. Kasyap, D. Sivakumar, and B. N. Raghunandan, “Flow and breakup characteristics of elliptical liquid jets,” International Journal of Multiphase Flow, vol. 35, no. 1, pp. 8–19, 2009.

7. L. Wang, X. Liu, and Z. Liu, “Evolution of low-aspect-ratio rectangular synthetic jets,” Physics of Fluids, vol. 30, no. 10, p. 107102, 2018.

8. A. Morad, A. Boudjemaa, and M. Benmouiza, “Three-dimensional numerical investigation of axis-switching and turbulence dynamics in rectangular jets,” International Journal of Multiphase Flow, vol. 126, p. 103242, 2020.

9. M. Smith and A. Glezer, “The formation and evolution of synthetic jets,” Physics of Fluids, vol. 10, no. 9, pp. 2281–2297, 1998.

10. L. D. Kral, A. T. Donovan, M. D. Bower, and A. Glezer, “Numerical simulation of synthetic jet actuators,” AIAA Journal, vol. 38, no. 3, pp. 354–362, 2000.

APPENDIX- 1

Component	Specification	Image
SJ actuator (Loudspeaker)	**Make:** Dynavox & Visaton; **Model:** LW5002PPR-S-M01 & FRS 8; **Rated power:** 60 & 30Watts; **Impedance:** 8 ohms	
Power oscillator	**Make:** Syscon Instrument; **Model:** SI28-DR; **Rated power:** 0 to 150 Watts; Frequency response:1 Hz to 10kHz	
Variable DC power Supply (Aplab 3260)	**Make:**Aplab; Model: L3260; **Max Voltage:** 32V; **Max Current:** 60A	

IR thermal imaging camera	**Make:** FLIR; **Model:** A655sc; Uncooled microbolometer detector array; **Range:**0-2000^{o}C	
Constant Temperature anemometer	**Make:** Dantec Dynamics; **Model:** Mini-CTA 54T42; **Probe:** 55P16; **Velocity range:** up to 50m/s	
Function generator	**Make:** Tektronix; **Model:** AFG 1022; **Frequency:** 0-20MHz	
Oscilloscope	**Make:** Tektronix; **Model:** TBS 1072B; **Frequency:** 0-75MHz	

Digital multimeter	**Make:** Fluke; **Model:** 287 True-RMS; **Range:** 50 mV-1000V; 500μA- 10A